

Supporting Information

Stabilization of Poly (methyl methacrylate) Nanofibers with Core-Shell Structures Confined in AAO Templates by the Balance between Geometric Curvature, Interfacial Interactions and Cooling Rate

Chen Zhang, Linling Li, Xiaoliang Wang*, and Gi Xue

Key Laboratory of High Performance Polymer Materials and Technology of Ministry of Education,
Department of Polymer Science and Engineering, School of Chemistry and Chemical Engineering,
State Key Laboratory of Coordination Chemistry, Nanjing National Laboratory of Microstructures,
Nanjing University, Nanjing 210093, P. R. China

*Correspondence Author: wangxiaoliang@nju.edu.cn

Thermogravimetric analysis (TGA)

To calculate the mass fractions of PMMA filled in AAO templates with different pore sizes, TGA measurement was carried out on the Perkin-Elmer TGA-Pyris system. All samples were heated from 25 to 700 °C at 10 K/min under nitrogen atmosphere. The TGA results for the bulk PMMA, the PMMA-filled AAO samples are shown in Figure S1.

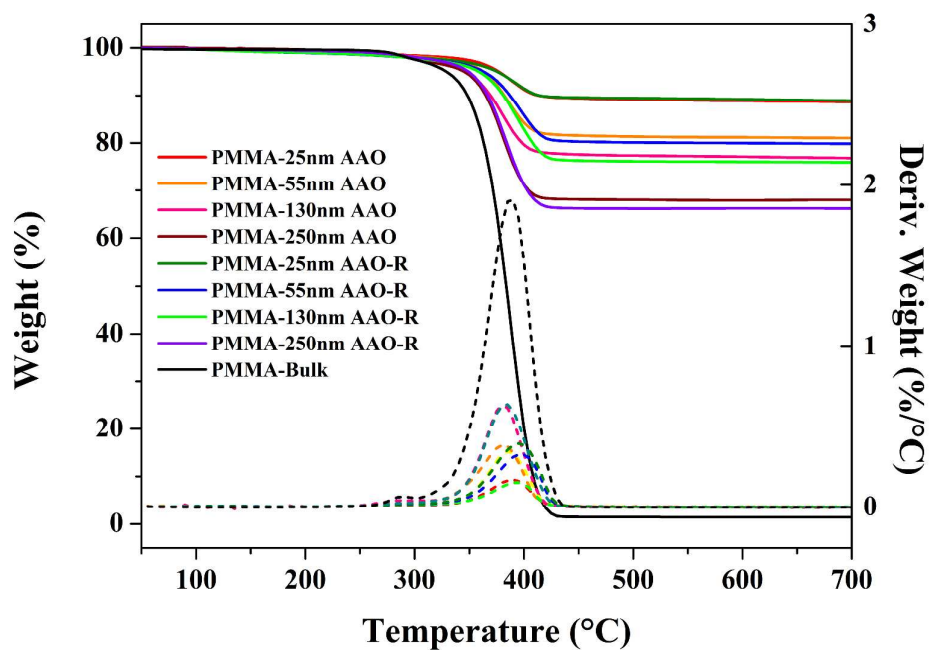


Figure S1. TGA thermograms of PMMA bulk, and PMMA in the pristine and surface modified AAO at a heating rate of 10 °C /min. The solid lines represent the TGA curves, and the dash lines represent the first derivative of the TGA curves.

Broadband Dielectric Spectroscopy (BDS)

Figure 2S shows the dielectric loss spectra as a function of frequency at different temperatures (80–160 °C) for bulk PMMA and PMMA confined in pristine AAO and surface-modified AAO templates. All AAO samples were firstly cooled from 180 to 30 °C at very slow cooling rate to make sure the complete formation of core-shell structure, and then heated from 30 to 180 °C.

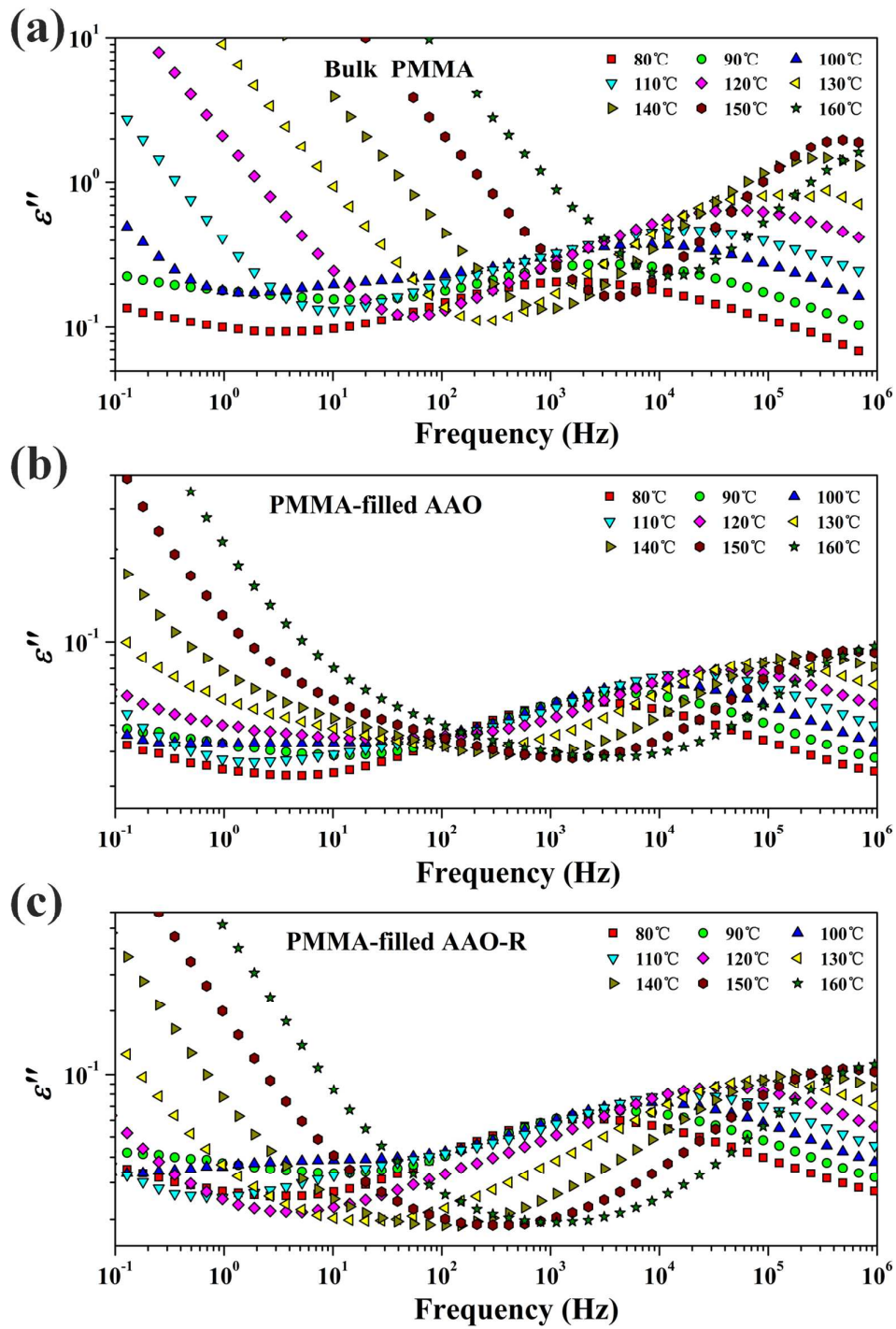


Figure S2. Dielectric loss (ϵ'') versus frequency at the indicated temperatures for (a) bulk PMMA, PMMA infiltrated into (b) pristine AAO and (c) modified AAO-R templates with 55 nm nanopores.

Contact Angles Measurements

To confirm the surface modification, contact angles of water on pristine and modified AAO templates were determined by an optical contact angle measuring device, as shown in Figure S3. Although the influence of alumina nanopore existence on contact angle could not be avoided considering that the AAO templates are open on both ends, the increased water contact angles indicate the modified AAO's surface changes to hydrophobic. The values of water contact angle are compiled in Table SI

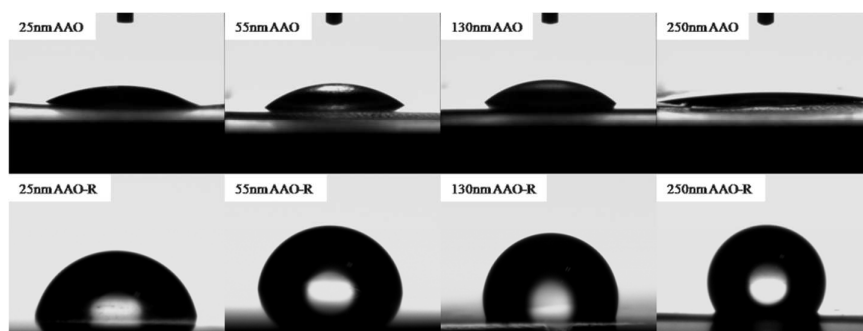


Figure S3. Contact angles of water on the pristine AAO template (first row) and the HMDSO-modified AAO template (second row).

TABLE SI. Contact angles (deg) of water on AAO and AAO-R templates

pore diameter	250 nm	130 nm	55 nm	25 nm
pristine AAO	11.4 (± 2.1)	41.3 (± 1.0)	32.0 (± 1.6)	23.5 (± 0.8)
modified AAO-R	122.9 (± 1.8)	102.4 (± 1.4)	90.8 (± 0.9)	78.8 (± 1.2)

DSC Results of Samples Suffering Ultraslow Cooling Rate at 0.1K/min

Two distinct T_g s were also detected for PMMA-filled AAO-R samples, as show in Figure S4a, and there are almost no differences between the glass transitions temperatures of PMMA confined in pristine AAO and modified AAO-R templates, as shown in Figure S4b.

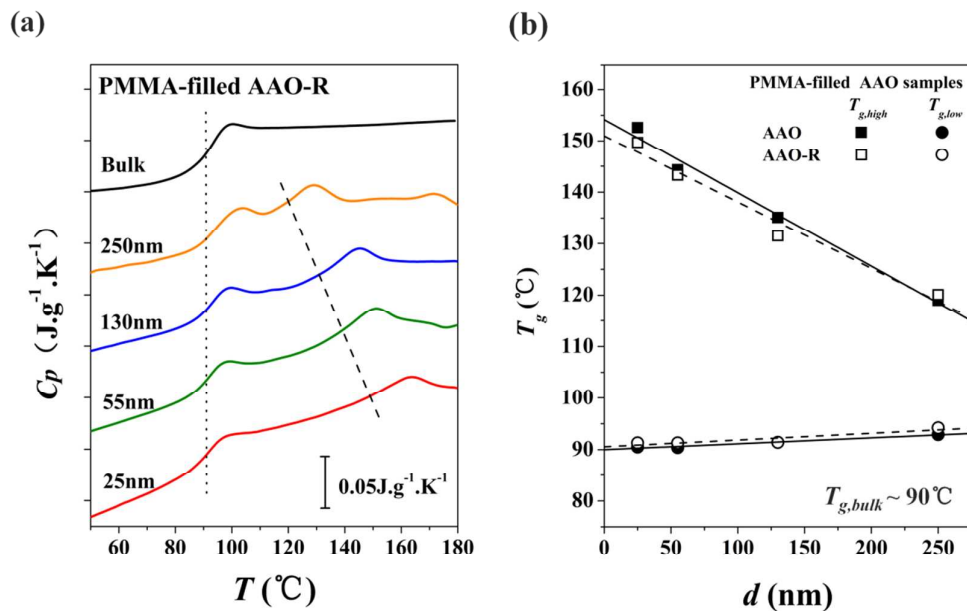


Figure S4. (a) Normalized DSC heating traces of PMMA filled in the modified AAO templates with different pore sizes. All samples were firstly cooled from 180 to 30 $^{\circ}C$ at 0.1 K/min to ensure the complete formation of core-shell structure, and then heated at 10 K/min. The DSC curves were normalized on the basis of the TGA results. (b) The double T_g s of confined PMMA in modified AAO-R and pristine AAO templates as a function of nanopore diameter d .

Differences in Interfacial Segmental Dynamics

To compare the differences of segmental dynamics between PMMA-filled AAO-R and the PMMA-filled AAO samples. BDS fitting curves of the PMMA-filled AAO-R samples were carried out, as shown in Figure S5. Temperature dependence of relaxation times for the PMMA confined in the surface-modified AAO templates and low-frequency slope, m , corresponds to the segmental relaxation are shown in Figure S6, associated fitting parameters are shown in Table SII.

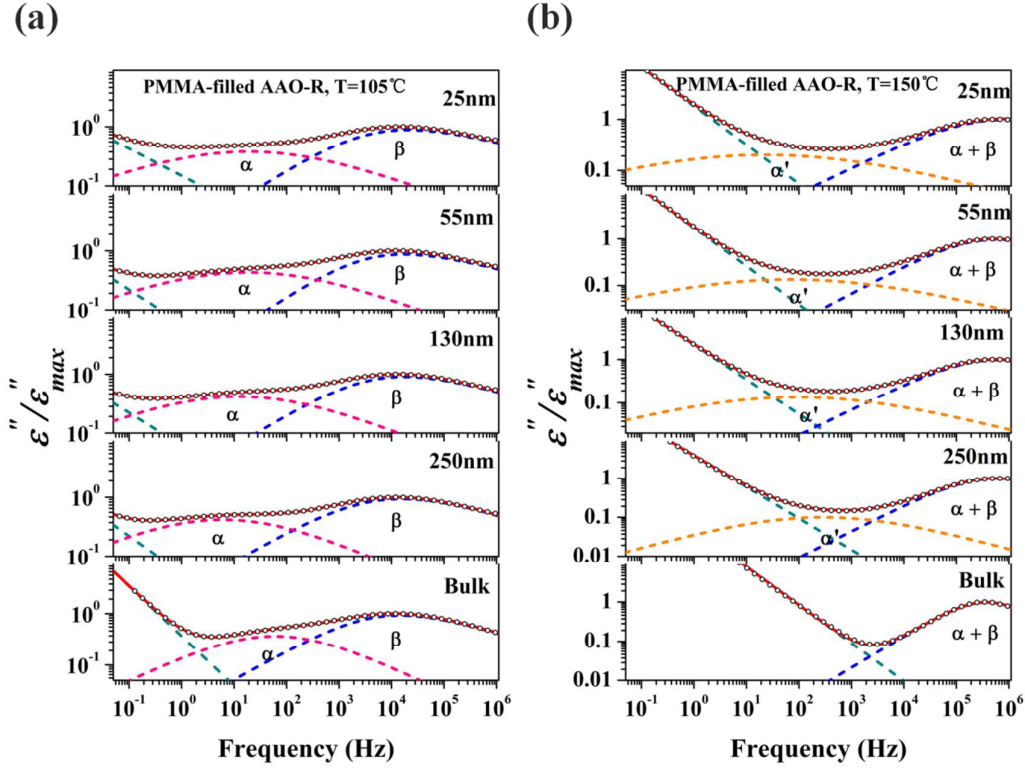


Figure S5. Frequency dependence of the normalized dielectric loss ε'' for bulk PMMA and PMMA confined in modified AAO-R templates with different diameters (25, 55, 130 and 250 nm) at (a) 105 °C and (b) 150 °C. The black circles represent the measurement data, the red solid lines represent the HN fitting curve, and the dashed lines represent the individual processes (the olive dashed lines the conductivity contribution).

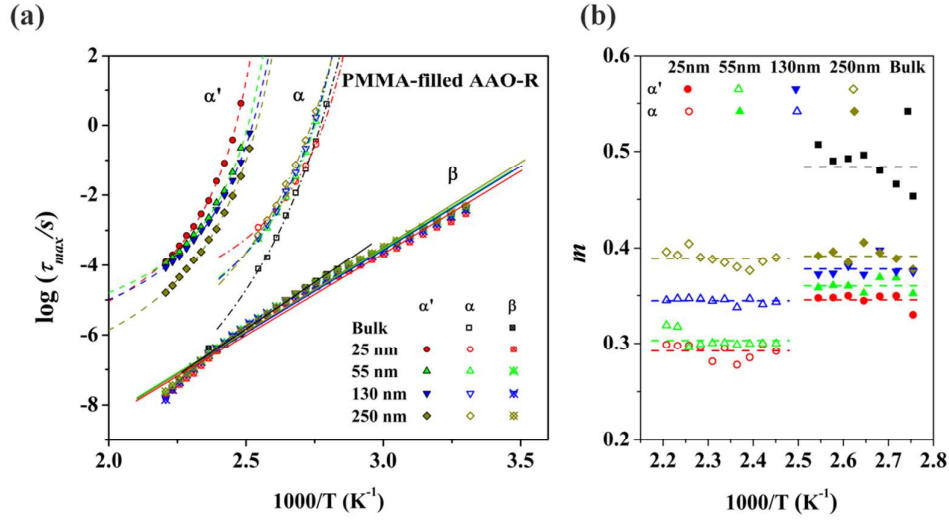


Figure S6. (a) Characteristic relaxation time τ_{max} as a function of reciprocal temperature for α' , α and β relaxations of bulk PMMA and PMMA confined in modified AAO-R templates with different pore sizes. The dashed lines correspond to α' VFT fittings, dash-dotted lines to α VFT fittings and solid lines to β Arrhenius fittings. (b) The low-frequency slope m corresponds to the segmental relaxation of the bulk (black squares) and the confined PMMA in modified AAO templates.

Table SII. VFT parameters of α' and α relaxation for PMMA-filled AAO-R templates

	α relaxation			α' relaxation		
	D	T_0/K	$T_g/^\circ C$	D	T_0/K	$T_g/^\circ C$
Bulk	6.1	297	78.9			
250 nm	4.4	306	82.4	2.4	350	112.2
130 nm	2.6	320	82.4	1.8	356	114.3
55 nm	2.1	324	82.3	1.5	363	117.5
25 nm	1.7	322	77.4	1.8	366	124.4

Cooling Rate Dependence

The evolution of nanofibers with core-shell structures confined in pristine AAO and AAO-R templates with different pore diameter is investigated by cooling rate experiments. The detailed DSC results are shown in Figure S7 and S8.

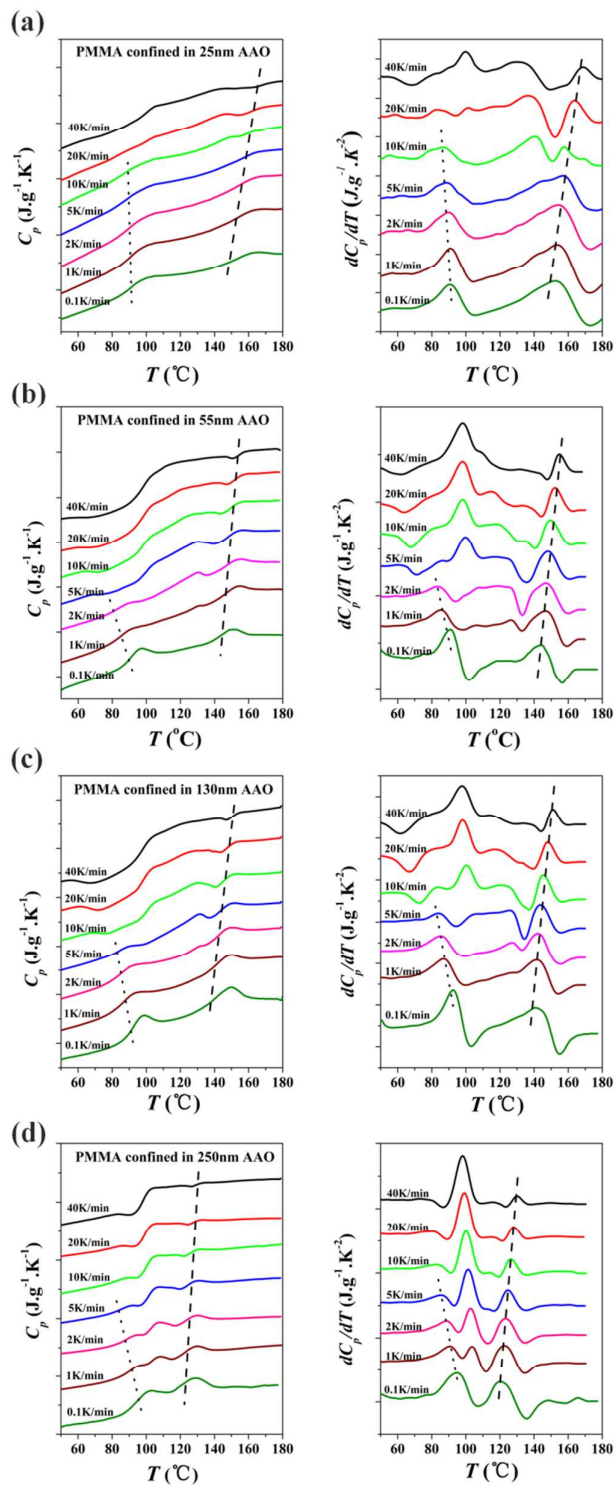


Figure S7. DSC heating traces of PMMA confined in pristine AAO templates with different nanopore size suffering different cooling rates across the T_g , and temperature derivative of the heat capacity curves: (a)25 nm, (b)55 nm, (c)130 nm, (d)250 nm. The dashed and dotted lines in these figures are guides for the eye.

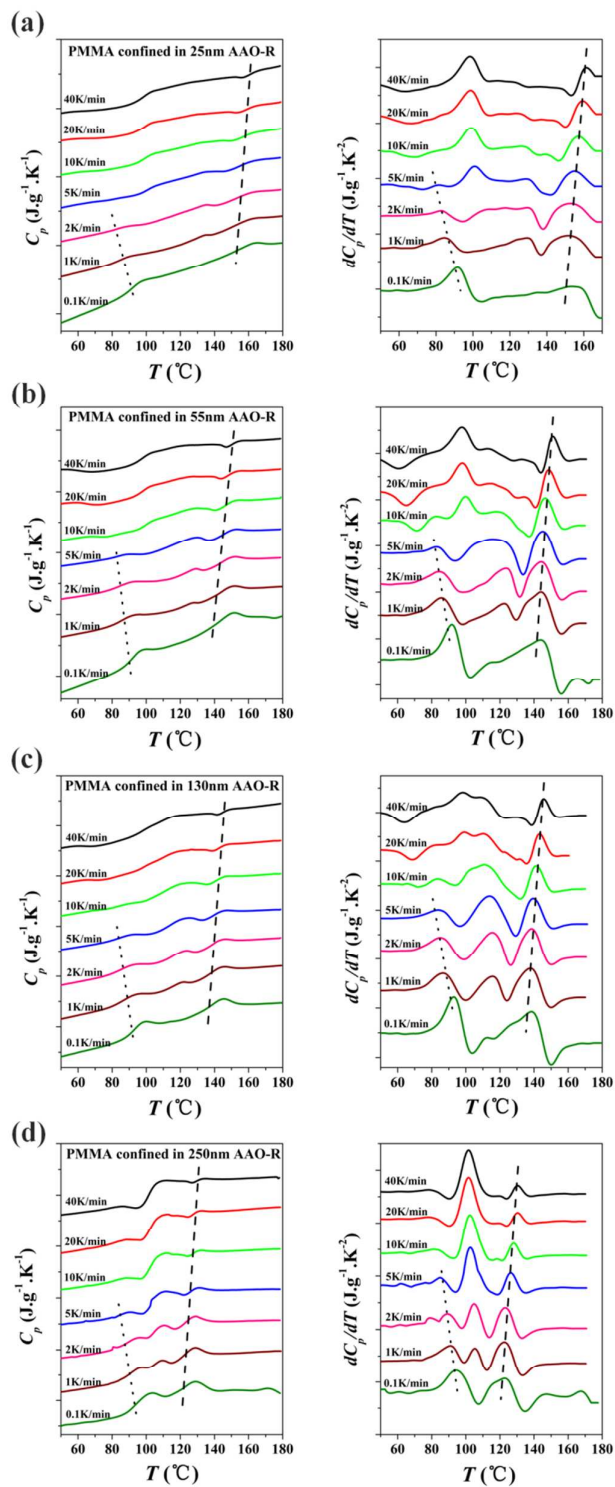


Figure S8. DSC heating traces of PMMA confined in modified AAO-R templates with different nanopore size suffering different cooling rates across the T_g and temperature derivative of the heat capacity curves: (a)25 nm, (b)55 nm, (c)130 nm, (a)250 nm. The dashed and dotted lines in these figures are guides for the eye.